Measurement of Photoneutron Yields Using the RPI LINAC and Assessment of Evaluated Photoneutron Data for Tantalum and Beryllium

Brian Epping[1,2*], *Michael* Rapp[1], *Devin* Barry[1], *Adam* Daskalakis[1], *Yaron* Danon[3], *Ezekiel* Blain[3], *Peter* Brand[3], *Michael* Bretti[3], *Matthew* Gray[3], *Larry* Krusieski[3], *Azeddine* Kerdoun[3], *Robert* Block[3], and *Sheldon* Landsberger[2],

[1]Naval Nuclear Laboratory, P.O. Box 1072, Schenectady, New York, 12301, USA
[2]University of Texas at Austin, Nuclear Engineering Teaching Laboratory, Pickle Research Campus, R-9000, Austin, Texas, 78712, USA
[3]Rensselaer Polytechnic Institute, Gaerttner LINAC Center, 110 8th Street, Troy, New York, 12180, USA

Abstract. A new experiment configuration was designed, developed, and implemented to measure photoneutron yields using the Rensselaer Polytechnic Institute (RPI) electron linear accelerator (LINAC) at the RPI Gaerttner LINAC Center. The experiment configuration includes a new target assembly that converts the LINAC electron beam into a high energy bremsstrahlung photon flux incident upon a sample material of interest. The photons excite nuclei in the sample of interest, which can subsequently emit neutrons (photoneutrons). The photoneutrons emitted in the direction of the detector system travel through a series of collimated vacuum pipes before reaching a pair of proton-recoil high-energy neutron detectors. The signals generated by the neutron detectors are processed using a digital data acquisition system and subsequently analyzed to determine the energy-dependent photoneutron yield from the sample of interest. The new experiment configuration was used to perform proof-of-concept experiments to measure the photoneutron yields from samples of tantalum and beryllium. The measured results were then compared against the results from Monte Carlo simulations of the detailed experiment configurations to perform preliminary assessments of evaluated photoneutron data libraries.

1 Introduction and Background

The Rensselaer Polytechnic Institute (RPI) electron linear accelerator (LINAC) is primarily used in support of neutron cross section measurements. The LINAC produces up to a 60 MeV electron beam which strikes a water-cooled tantalum target, creating a bremsstrahlung photon flux that excites the tantalum nuclei and results in the emission of neutrons. Neutrons traveling in the direction of samples of interest pass through collimated evacuated pipes. Various detector systems are used to measure the neutron interaction rates in the samples and allow subsequent determination of cross sections.

Work efforts at the RPI LINAC often require simulation of the specific experimental configurations using neutron transport codes such as the Monte Carlo particle transport code, MCNP [1]. It has long been known that such simulations starting with the electron beam incident on the target do not produce the correct neutron emission spectra [2]. One potential cause is inaccuracies in the photoneutron data libraries used in the simulations. This project endeavoured to demonstrate a proof-of-concept experimental configuration to interrogate the performance of evaluated photoneutron data libraries using experimentally measured data. A high level summary of the project efforts and results are summarized in the following sections. Additional details regarding the experimental configuration development, equipment used, experiments performed, and data analysis methods utilized are documented in [3].

2 Experimental Configuration

2.1 Basic Experimental Configuration

A new experiment configuration was developed for use at the RPI LINAC to measure photoneutron yields from samples of interest. In this configuration, the LINAC electron beam is directed onto a bare tantalum plate (converter), which converts the electron beam into a bremsstrahlung photon flux. Residual electrons that emerge from the converter are swept away by a dipole magnet to ensure they do not contact the sample and instead are fully absorbed in an aluminium beam dump. A sample of interest is placed in the flight path of the photon flux and photoneutrons are induced when the photons strike the sample. Collimated evacuated pipes are positioned to provide a clear flight path for photoneutrons emitted from the sample toward the detection system (at an angle of 90 degrees from the initial electron beam direction). The detection system

* Corresponding author: brian.epping@unnpp.gov

consists of two neutron detectors located at a distance of approximately100 meters from the sample, along with the supporting components and electronics necessary to record the data. Data are recorded in various time bins correlated to each LINAC pulse to allow determination of the energy of each neutron event using the time of flight method [4]. Each detection event is digitized for subsequent data processing and analysis. An illustration of the basic experimental configuration is shown in Fig. 1.

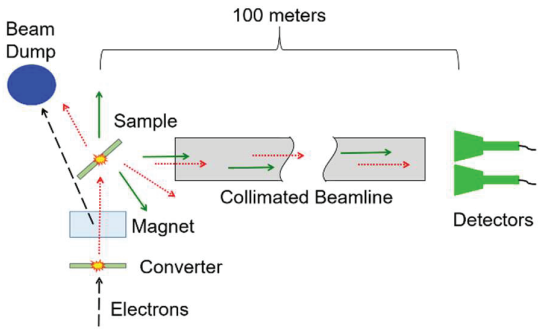

Fig. 1. Basic representation (not to scale) of the experimental configuration used to measure photoneutron yields at the RPI LINAC. The black dashed arrows represent the LINAC electron beam and residual electrons emerging from the converter. The red dotted arrows represent photons emitted by the converter and the sample. The green solid arrows represent neutrons emitted from the sample.

2.2 Developmental Experiments

Several developmental experiments were performed in order to investigate and validate the new measurement configuration.

The first set of experiments used radiochromic film (without the converter in position) to map the LINAC electron beam traversing through and ultimately exiting the dipole magnet towards the beam dump to ensure that any residual electrons ultimately emitted by the converter would be sufficiently swept away to avoid striking the sample and be fully absorbed in the beam dump. An additional set of radiochromic film measurements was performed with the converter in position to verify that the photon flux emitted by the converter would strike the sample.

The second set of experiments measured residual electrical currents in various components in an attempt to correlate the magnitude of the LINAC electron beam (which cannot be directly determined during measurements) for eventual use in normalizing MCNP simulation results to the actual experimental conditions. Unfortunately, these efforts were not successful, resulting in the need to use a more generalized normalization technique as discussed in section 3.3.

The third set of experiments monitored the temperatures of the converter, beam dump, and sample during maximum power LINAC operation to ensure that these components would not overheat and suffer damage.

The final set of experiments was used to characterize the efficiency of the neutron detectors. These efforts were only partially successful, and ultimately resulted in the need to re-utilize previously determined detector efficiency values from another project [5].

3 Photoneutron Measurements and Analysis

3.1 LINAC Experiment Runs

The new experimental configuration was used to measure photoneutron yields for tantalum and beryllium using the RPI LINAC. Each experimental run lasted approximately one week. In addition to measuring the photoneutron yield from the tantalum and beryllium samples, additional data runs were performed using an open (i.e., no sample) position to assist in characterizing the background as well as additional runs using a graphite (carbon) filter inserted in the neutron beam to determine the effective neutron flight path length. The applicable details of the experiment conditions (materials, detailed geometries, LINAC operating conditions, etc.) were recorded for use in the subsequent Monte Carlo simulations.

3.2 Analysis of Measured Data

Pulse shape analysis [5] was used to identify neutron events in the detectors and eliminate gamma ray photon events. The neutron events were then summed for each individual time bin.

The summed neutron counts were corrected for background. The background signal consists of two parts: the time-independent (LINAC off) background and the time-dependent background which results from LINAC operation. The time-independent background was determined by recording detector events over a period of a few days while the LINAC was not operating – the results demonstrated that the time-independent background was negligibly small and could be ignored. The time-dependent background was determined by measuring neutron events while the LINAC was pulsing but there was no sample material in position downstream from the converter. These “open sample” neutron counts were run-time normalized and subtracted from the measured sample neutron counts to eliminate the background.

Observing the time bin spacing between known resonances in the neutron transmission through the carbon filter allowed the neutron flight path length between the sample and detectors to be determined (101.4 meters). The location in time of the “gamma flash” (i.e., the burst of gamma ray photons that coincides with neutron emission from the sample) was then used in conjunction with the flight path length to establish “time zero” (i.e., the time bin corresponding to when each photon pulse impinged upon the sample). The time zero and flight path length were then used to define the actual time grid for the neutron flight from each LINAC pulse and the corresponding neutron energies for each detector time bin via the time of flight

method. Finally, a smoothing algorithm was used to minimize bin-to-bin variations in the photoneutron yield results.

The relative uncertainties for all known experimental effects were propagated through to the results shown in section 4.

3.3 Monte Carlo Simulations

The detailed experiment conditions recorded during the measurement runs were used to develop and execute MCNP simulations of the experiments. The ENDF/B-VIII.0 nuclear data library was used during the simulations for the transport of all particles through all materials with the exception of photoneutron emission from the sample of interest, for which the specific libraries being assessed in this study were varied from run-to-run as applicable.

Since the measurements of correlation of residual currents described in section 2.2 were inconclusive, there was no absolute method available to normalize the MCNP "per source particle" results to the measured results based on LINAC electron beam current. As a work-around for this preliminary study, the MCNP results were area-normalized to the measured results. Therefore, the relative shapes of the measured versus simulated results could be compared (although the absolute values could not).

The relative uncertainties from the MCNP output decks were propagated through to the results shown in section 4.

4 Results

The measured photoneutron data results for tantalum are compared to MCNP simulations using two evaluated photoneutron libraries (ENDF/B-VIII.0 [6, 7, 8] and IAEA-2019 [9]) in Figures 2 and 3. Fig. 2 shows that the measured data and both libraries are in good general agreement up to approximately 3 MeV. Fig. 3 suggests that both libraries may be under-predicting the photoneutron emission from tantalum in the energy range of 3 MeV – 12 MeV, with the IAEA-2019 performing generally better than ENDF/B-VIII.0 between 3 MeV and 6.5 MeV. However, it should be noted that limitations in the ability for MCNP to account for anisotropic emission of photoneutrons may also be a contributor to the observed mismatches between the measured and simulated results in this energy range [10].

The measured photoneutron data results for beryllium are compared to MCNP simulations using two evaluated photoneutron libraries (IAEA-1999 [11] and IAEA-2019) in the energy range of 0.5 MeV to 6 MeV in Fig. 4. Both libraries have variations not seen in the measured data results, with the IAEA-1999 showing large variations between 2.5 MeV and 3.5 MeV. The IAEA-2019 library has better general agreement with the measured data results over the entire energy range.

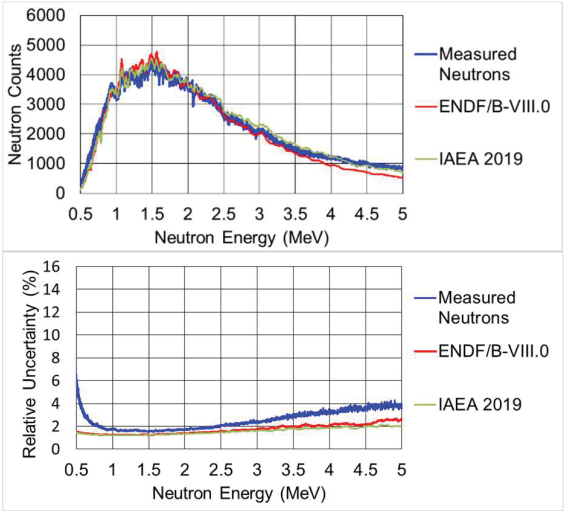

Fig. 2. Comparison of measured photoneutron yield from tantalum over the energy range of 0.5 MeV to 5 MeV to MCNP simulation results using the photoneutron libraries from ENDF/B-VIII.0 and IAEA 2019. Relative uncertainties are shown in the lower graph. Uncertainties in the simulations only represent the statistical uncertainties.

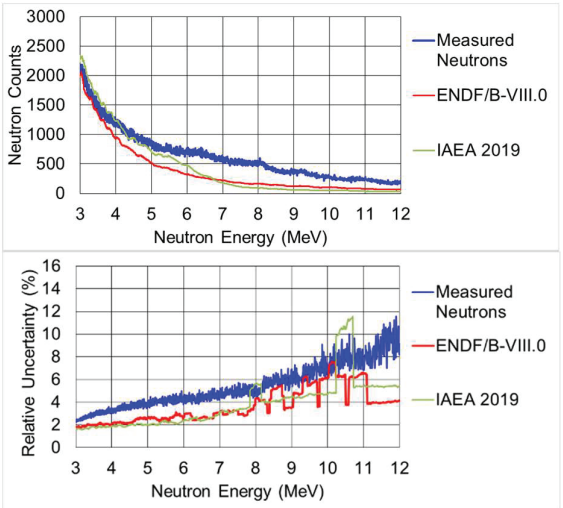

Fig. 3. Comparison of measured photoneutron yield from tantalum over the energy range of 3 MeV to 12 MeV to MCNP simulation results using the photoneutron libraries from ENDF/B-VIII.0 and IAEA 2019. Relative uncertainties are shown in the lower graph. Uncertainties in the simulations only represent the statistical uncertainties.

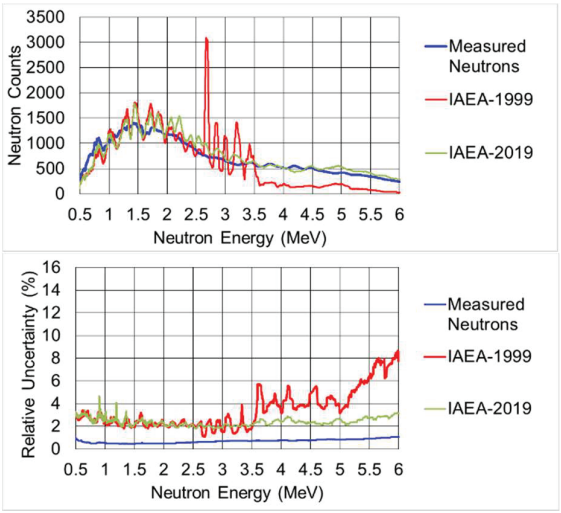

Fig. 4. Comparison of measured photoneutron yield from beryllium over the energy range of 0.5 MeV to 6 MeV to MCNP simulation results using the photoneutron libraries from IAEA-1999 and IAEA-2019. Relative uncertainties are shown in the lower graph. Uncertainties in the simulations only represent the statistical uncertainties.

5 Conclusions

The capability to use the RPI LINAC to measure photoneutron yields and then analyze the data to assess the performance of evaluated photoneutron data libraries has been demonstrated as a proof-of-concept. The results obtained thus far are only preliminary, due to known limitations with the current experiment configuration (including but not limited to, inability to perform detailed characterization of the LINAC electron beam operating conditions and the efficiencies of the neutron detectors). Future upgrades to the RPI LINAC and the photoneutron experiment configuration and methods are in progress and expected to provide higher quality results. Upon completion of the upgrades, plans are in place to repeat the tantalum and beryllium photoneutron measurements, perform comprehensive assessments, and publish the final results.

References

1. J.T. Goorley, M.R. James, T.E. Booth, F.B. Brown, J.S. Bull, L.J. Cox, J.W. Durkee Jr., J.S. Elson, M.L. Fensin, R.A. Forster III, J.S. Hendricks, H.G. Hughes III, R.C. Johns, B.C. Kiedrowski, R.L. Martz, S.G. Mashnik, G.W. McKinney, D.B. Pelowitz, R.E. Prael, J.E. Sweezy, L.S. Waters, T. Wilcox, and A.J. Zukaitis, LA-UR-13-22934 (2013)
2. F.J. Saglime III, *High Energy Nuclear Differential Scattering Measurements for Beryllium and Molybdenum*, Ph.D. Thesis, Rensselaer Polytechnic Institute (2009)
3. B.E. Epping, *Measurement of Absolute Neutron Yields and Energy Spectra Using the RPI LINAC and Assessment of Evaluated Photoneutron Data for Tantalum*, Dissertation, University of Texas at Austin (2020)
4. M.J. Rapp, *Design and Construction of a Large Area Detector System and Neutron Total Cross Section Measurements in the Energy Range 0.4 to 20 MeV*, Ph.D. Thesis, Rensselaer Polytechnic Institute (2011)
5. A.M. Daskalakis, *Measurement of Elastic and Inelastic Neutron Scattering in the Energy Range from 0.5 to 20 MeV*, Ph.D. Thesis, Rensselaer Polytechnic Institute (2015)
6. D.A. Brown, M.B. Chadwick, R. Capote, A.C. Kahler, A. Trkov, M.W. Herman, A.A. Sonzogni, Y. Danon, A.D. Carlson, M. Dunn, D.L. Smith, G.M. Hale, G. Arbanas, R. Arcilla, C.R Bates, B. Beck, B. Becker, F. Brown, R.J. Casperson, J. Conlin, D.E. Cullen, M.A. Descalle, R. Firestone, T. Gaines, K.H. Guber, A. Hawari, J. Holmes, T.D. Johnson, T. Kawano, B.C. Kiedrowski, A.J. Koning, S. Kopecky, L. Leal, J.P. Lestone, D. Márquez, C.M. Mattoon, E.A. McCutchan, S. Mughabghab, P. Navratil, D. Neudecker, G.P.A. Nobre, G. Noguere, M. Paris, M.T. Pigni, A.J. Plompen, B. Pritychenko, V.G. Pronyaev, D. Roubtsov, D. Rochman, P. Romano, P. Schillebeeckx, S. Simakov, M. Sin, I. Sirakov, B. Sleaford, V. Sobes, E.S. Soukhovitskii, I. Stetcu, P. Talou, I. Thompson, S. Van der Marck, L. Welser-Sherrill, D. Wiarda, M. White, J.L. Wormald, R.Q. Wright, M. Zerkle, G. Žerovnik, Y. Zhu, Nucl. Data Sheets **148**, pp. 1-142 (2018)
7. M.B. Chadwick, P.G. Young, S. Chiba, S.C. Frankle, G.M. Hale, H.G. Hughes, A.J. Koning, R.C. Little, R.E. MacFarlane, R.E. Prael, and L.S. Waters, Nucl. Sci. Eng. **131**, No. 3, pp. 293-328 (1999)
8. M.B. Chadwick, P.G. Young, R.E. MacFarlane, M.C. White, and R.C. Little, Nucl. Sci. Eng. **144** No. 2,, pp. 157-173 (2003)
9. T. Kawano, Y.S. Cho, P. Dimitriou, D. Filipescu, N. Iwamoto, V. Plujko, X. Tao, H. Utsunomiya, V. Varlamov, R. Xu, R. Capote, I. Gheorghe, O. Gorbachenko, Y.L. Jin, T. Renstrom, M. Sin, K. Stopani, Y. Tian, G.M. Tveten, J.M. Wang, T. Belgya, R. Firestone, S. Goriely, J. Kopecky, M. Krtička, R. Schwengner, S. Siem, M. Wiedeking, Nucl. Data Sheets **163**, pp. 109-162 (2020)
10. M. Rising, C.J. Josey, and W. Haeck, LA-UR-22-21663, *Photonuclear Physics Options in the MCNP6 Transport Code,* in Workshop for Applied Nuclear Data Activities (WANDA 2022), Feb. 28 – Mar. 4, 2022
11. P. Oblozinski, ed., *Handbook on Photonuclear Data for Applications Cross-sections and Spectra, Final report of a co-ordinated research project 1996-1999*, IAEA TECDOC No. 1178, (2000)